Available online at www.sciencedirect.com
ScienceDirect
Journal of Nuclear Materials 374 (2008) 298–303
journal of nuclear materials
www.elsevier.com/locate/jnucmat

Mechanical properties of V–4Cr–4Ti strengthened by precipitation and cold rolling

J.M. Chen [a,c,*], T. Nagasaka [b], T. Muroga [b], S.Y. Qiu [c], C. Li [c], N. Nita [d]

[a] Southwestern Institute of Physics, P.O. Box 432, Chengdu 610041, China
[b] National Institute for Fusion Science, Oroshi, Toki, Gifu 509-5292, Japan
[c] National Key Laboratory for Nuclear Fuel and Materials, P.O. Box 436, Chengdu 610041, China
[d] Institute for Materials Research, Tohoku University, 2-1-1 Katahira, Sendai 980-8577, Japan

Received 6 March 2007; accepted 23 August 2007

Abstract

V–4Cr–4Ti (NIFS-Heat-2) was strengthened in a thermo-mechanical process in which the alloy was solution-annealed at 1100 °C for 1 h and then aged at 600 °C for 20 h, followed by cold rolling at room temperature with a reduction of 20% in thickness. TEM observation indicated that extremely fine precipitates were produced during the aging. Precipitate coarsening did not occur during annealing the alloy at 750 °C due to the existence of high number density dislocations in the cold rolled alloy. High-temperature tensile tests showed this strengthening could remain effective up to 750 °C. Uniaxial thermal creep tests were conducted at 700–800 °C. Improvement in the property was observed at high stress level.

PACS: 28.52.Fa; 81.05.Bx; 62.20.−x; 81.40.Ef

1. Introduction

V–4Cr–4Ti is considered as the leading structural material of the V–Li blanket in a fusion reactor. One of its major advantages over other steel blankets is its high operation temperature and the resulting high thermal efficiency. The upper operation temperature limit, determined by high-temperature tensile strength and creep strength of the material, is about 650 °C for V–4Cr–4Ti [1]. For higher efficiency, further strengthening should be considered. One way is to add more Cr into the alloy, such as the high-Cr alloys recently investigated [2]. However, results showed that the addition should not exceed 7% in mass, since higher Cr content increased DBTT (ductile–brittle transition temperature) significantly. Adding W to the alloy seemed promising as has been generally considered for low activation ferritic steels. However, results showed no improvement of high-temperature tensile strength for V-base alloys [3]. Therefore, other ways than alloying should be considered for strengthening.

V–4Cr–4Ti could be strengthened by precipitation and cold rolling significantly [4]. It was found that fine Ti (CON) precipitates formed during aging at 600 °C strengthened the alloy with slight loss of ductility. But these precipitates were thermally unstable above 600 °C. Work hardening by cold rolling is another way for the strengthening. It may improve high-temperature creep strength as shown in 316 type steels [5]. For V–4Cr–4Ti, the dislocations introduced by cold rolling recovered above 600 °C [6]. Since fine precipitates could resist dislocation movement, with both precipitation and cold rolling, the thermal stability of the Ti (CON) precipitates and the dislocations may be enhanced due to their interaction.

In the present paper, the high-temperature properties of a V–4Cr–4Ti alloy (NIFS-Heat-2) were studied. The alloy

* Corresponding author. Address: Southwestern Institute of Physics, P.O. Box 432, Chengdu 610041, China. Tel.: +86 28 82850384; fax: +86 28 82850956.
E-mail address: chenjm@swip.ac.cn (J.M. Chen).

0022-3115/$ - see front matter © 2007 Elsevier B.V. All rights reserved.
doi:10.1016/j.jnucmat.2007.08.012

had been strengthened by precipitation and cold rolling (20% CW). The thermal stability of the precipitates and dislocations were examined. Creep tests were conducted with the analysis of the underlying mechanism.

2. Experimental procedures

The material used in this study was the V–4Cr–4Ti alloy of NIFS-Heat-2. Its chemical composition was shown in Ref. [4]. The as-received alloy plates were 0.5–1 mm thick and in the cold rolled state of >90% reduction in thickness. Tensile, creep specimens and TEM (transmission electron microscope) samples of 0.25 mm thick were cut from these plates after various thermo-mechanical treatments. At first, they were cold rolled to meet specimen thickness requirements, followed by heat treatments of solid-solution annealing (SA) and aging (A). The SA treatment was performed at 1100 °C for 1 h to dissolve most precipitates that had formed in the previous thermo-mechanical processes [7], while the aging (A) was conducted at 600 °C for 20 h. Alloy in the aging state was named as SAA. For further strengthening, SAA plates were cold rolled again, with a 20% reduction in thickness (SAACW). The plates followed the SAACW process were expected to contain fine precipitates and dislocations, both in high number density. For comparison study, a cold rolled plate was treated under the standard (STD) condition as annealed at 1000 °C for 2 h. The average grain size of the alloy in SAA and STD states was about 28 μm and 18 μm, respectively.

All of the heat treatments mentioned above were performed in a high vacuum furnace. The vacuum was better than 1×10^{-4} Pa. Samples or pieces of the plates were sandwiched with Ta plates and wrapped with Zr foil as a gaseous impurity getter. Heating rate was 20 °C/min. At finishing, power supply was turned off and the plates were cooled down to room temperature (RT) in the furnace in vacuum.

Specimens were cut or punched out from 0.25 mm thick plates. The tensile specimens, used as the creep test specimens, had the gauge dimension of $5 \times 1.2 \times 0.25$ mm^3. Samples for hardness test, $10 \times 5 \times 0.25$ mm^3 in dimension, were ground with sandpapers and polished by hand with plaster of Al_2O_3 and oil instead of water to avoid hydrogen pick-up. For microstructure analysis by transmission electron microscope (TEM), 3 mm diameter disks were prepared.

Tensile tests were performed at RT and 600–800 °C in vacuum of better than 1×10^{-4} Pa with the tensile test machine in Tohoku University. Initial strain rate was 6.67×10^{-4} s^{-1}. A specimen was kept at the test temperature for ~20 min before tensile test could begin. Creep test was conducted at 600, 750 and 800 °C in vacuum of $\sim 4 \times 10^{-5}$ Pa using an uniaxial creep test machine [8]. Uniaxial and constant load were applied to the specimen by load blocks. Zr foil acted as oxygen impurity getter surrounded the test specimen. Creep test started after the computer recorded load and displacement signals became stable, which took about 7 h. Vickers hardness test was performed at RT. Load was 3 N with duration of 30 s.

Tensile properties were measured from load–displacement curves, while the creep rates were obtained according to the steadily and linearly increasing displacement on time. As the cross-section area of the creep specimen was decreasing in the test due to creep deformation, the true stress applied on the specimen would increase with time. The true stress in the steady creep stage was averaged as the applied stress. The microstructures of the specimens before the tensile or creep tests were examined with TEM, and the fracture surface of the tensile specimen and the creep-tested specimen were analyzed with a scanning electron microscope (SEM). Observed also was the specimen surface after the creep test for examining grain structure.

3. Experimental results

3.1. Precipitation hardening and work hardening by cold rolling

As shown in Fig. 1(a), the hardening by aging the SA alloy at 600 °C was significant. Its hardness increased with increasing aging time. Fig. 1(b) shows that the hardness of the SAACW alloy was about 20% higher than that of the SAA alloy, showing the contribution of the 20% cold rolling to the hardening. The hardness of the alloy in both

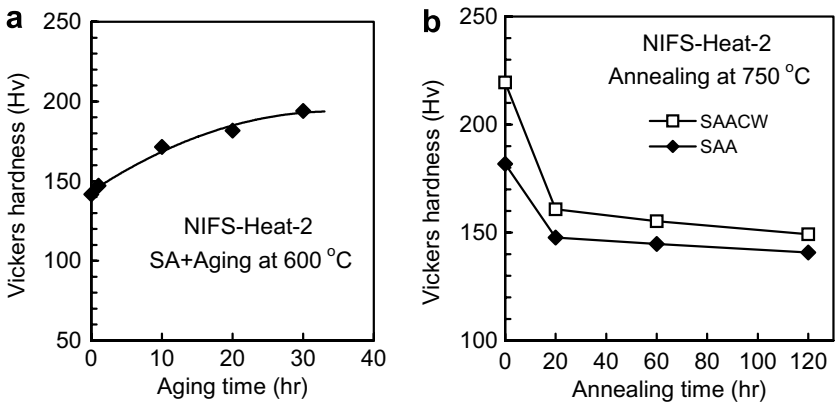

Fig. 1. Response of hardness on aging time (a) and annealing time (b). Aging and annealing temperature are indicated in the figure.

states decreased with time during the annealing at 750 °C. Following a rapid decrease in the initial 20 h, the hardness decreased much slowly thereafter. Invariably the SAACW alloy kept its higher hardness than the SAA alloy throughout the process.

Fig. 2 shows the TEM microstructure of the alloys after the annealing at 750 °C for 0, 20 and 60 h, respectively. For the SAA alloy without annealing, dim precipitates were observed. The precipitates were so fine that only obscure image could be obtained even in dark-field weak-beam imaging condition due to the insufficient resolution of the TEM. These fine precipitates, which hardened the alloy, grew as disks in the annealing as shown in the figure. The growth caused the decrease in its number density and in hardness as shown in Fig. 1(b). The disk-shaped precipitates were placed on the (0 0 1) plane. For the SAACW alloy, dislocation density decreased during the annealing, resulting in the decrease in hardness. Few precipitates were observed in the TEM images. However, high density fine precipitates should have existed in the alloy due to the ageing prior to the cold rolling like the case in SAA alloy. These precipitates, which could dimly be observed with the TEM as mentioned, hardly grew in the annealing at 750 °C, thus few precipitates could be observed due to its extremely small size even after the annealing for 60 h.

3.2. High-temperature tensile properties

Tensile results are shown in Fig. 3. Comparing to the alloy in STD state, SAA treatment caused the alloy some increase in yield strength (YS) and some loss of uniform elongation. Once again, the alloy in SAACW state displayed much higher yield strength than the alloy in other states up to 800 °C. On the other hand, the uniform elongation (UE) of the SAACW alloy was very small, indicating the big loss of strain hardening capability by the cold rolling. According to the temperature dependence shown in Fig. 3(c), some recovery of the capability appeared above 700 °C along with an accelerating decrease in the yield strength as shown in Fig. 3(a).

Temperature dependence of ultimate tensile strength (UTS) was similar to that of the yield strength (see Fig. 3(b)). The difference in UTS between the alloy in SAACW and STD states was not as large as that in YS, because of the smaller difference in YS and UTS of the SAACW alloy for its very smaller strain hardening capability than that of the STD alloy. Fig. 4 indicates the decrease of the tensile strengths of the SAACW alloy at 750 °C due to the annealing at 750 °C. This is consistent with the hardness loss as shown in Fig. 1(b). With the decrease in the strength, the uniform elongation increased after the annealing.

Despite the significant loss of uniform elongation, the SAACW alloy was considered to be ductile because the reduction of area was very high. Fig. 5 shows the SEM image of the fracture surface of the SAACW specimen tested at RT. The fractured area had a width of ~10 μm. According to the initial specimen thickness, the reduction of area was more than 90%. The SAACW alloy tested at other temperatures also showed reduction of area of exceeding 90%.

3.3. Creep test result

Typical thermal creep behavior is shown in Fig. 6, along with the applied stress beside the creep curve. It indicated

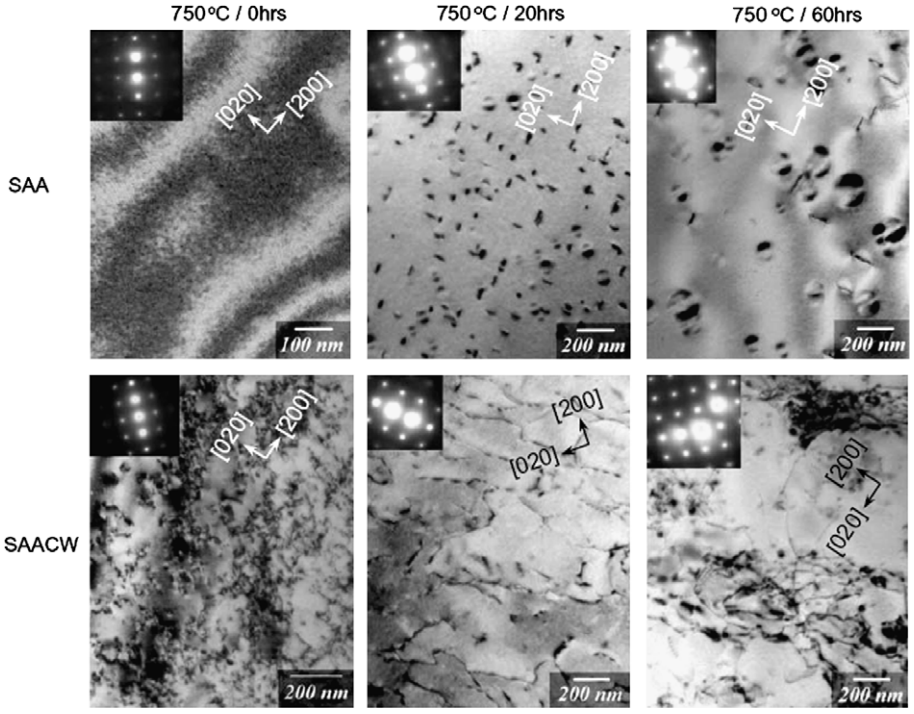

Fig. 2. TEM microstructure of the SAA and SAACW alloy after annealing at 750 °C.

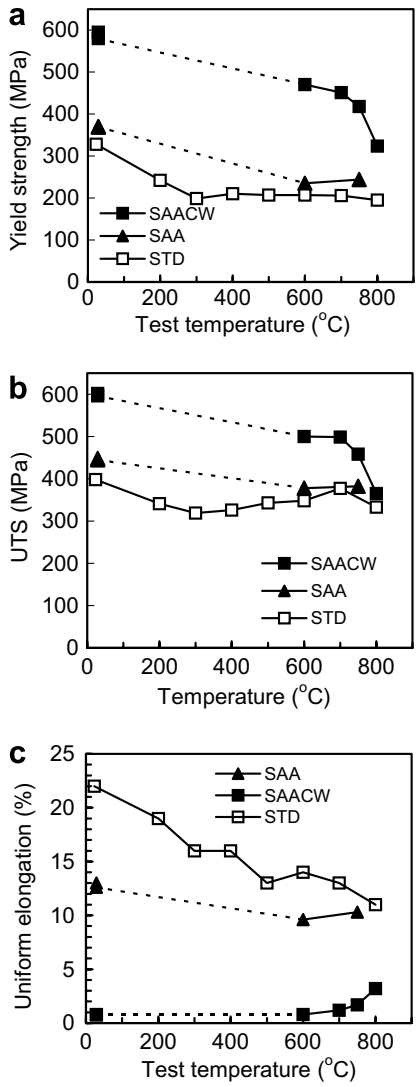

Fig. 3. The yield strength (a), ultimate tensile strength (UTS) (b) and uniform elongation (c) of the alloy in various thermo-mechanical states as a function of test temperature.

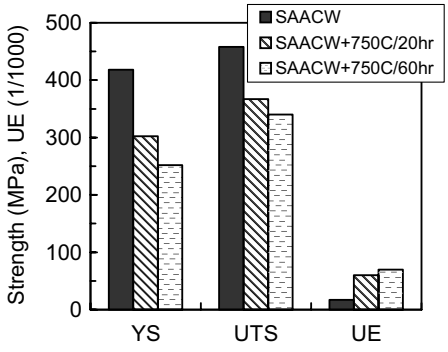

Fig. 4. The effect of annealing at 750 °C on the tensile properties measured at 750 °C.

that the rupture time of the SAACW alloy was longer than the STD alloy at 800 °C. The creep could approximately be divided into three stages. The primary creep stage, which

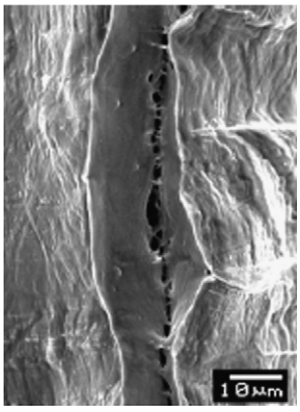

Fig. 5. SEM photo showing the fracture of the SAACW specimen tested at RT.

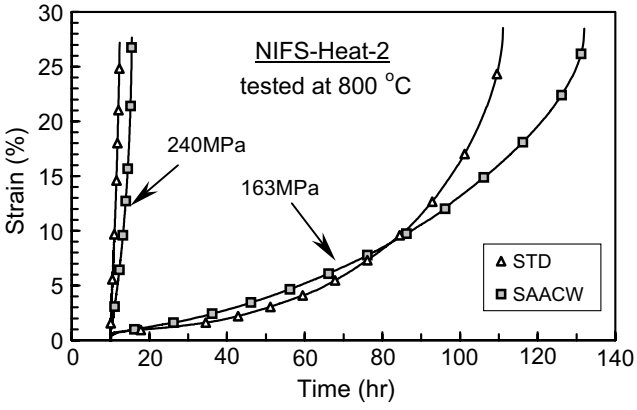

Fig. 6. Creep deformation behavior of NIFS-Heat-2 in STD and SAACW states.

was very short, had fast decreasing creep rate with time. The 2nd stage took longer time in which the alloy crept steadily and slowly. The maximum strain in this stage was usually less than 2%. Thereafter the creep got into the longest 3rd stage where the creep rate increased with time. As an example, for the STD alloy tested at 163 MPa and 800 °C, the three stages took about 1.6%, 13.3% and 85.1% of the rupture time, respectively.

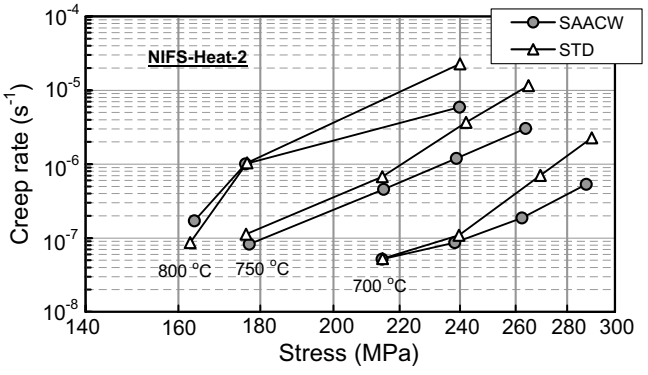

Fig. 7. Steady creep rate as a function of the applied stress at 700, 750 and 800 °C.

Fig. 7 shows the dependence of the steady creep rate on the applied stress for the STD and SAACW alloys tested at 700, 750 and 800 °C, respectively. The rate increased with increasing test temperature and applied stress. Beyond a certain stress level, the SAACW alloy exhibited lower creep rate than the STD alloy, indicating the improvement of the property by the aging and cold rolling. This critical stress seems to decrease with increasing test temperature. Below this stress, the alloy in both states showed similar creep rate.

4. Discussion

4.1. The thermally stable precipitates in the cold rolled alloy

Usually the fine Ti (CON) precipitates formed in V–4Cr–4Ti at 600–700 °C are thermally unstable above 500 °C where Ti becomes mobile [4]. This was partially verified in the present study due to the observed growth of the precipitates in the SAA alloy on annealing at 750 °C. However, the SAACW alloy containing fine precipitates showed no precipitate growth in the same annealing. It seems that dislocations introduced by cold rolling in the alloy could retard the precipitate growth. Definitely, precipitate growth requires the migration of the species forming the precipitate from the matrix to precipitates or from small precipitates to larger ones. So the diffusion seemed to be suppressed by dislocations in the SAACW alloy.

It was found that there is strong interaction between dislocations and interstitial solutes of C, N and O in V–4Cr–4Ti, which caused the dynamic strain aging (DSA) phenomenon and increased the flow stress of the alloy during tensile test at 300–750 °C [11]. This means that the interstitial solutes retarded the dislocation movement in the alloy even at 750 °C. On the other side the dislocations would exert equal resistance to the motion of the interstitial solutes at the same time. In the present study, similar interaction would occur due to the movement of the dislocations in the hardness recovery process of the SAACW alloy. It should account for the non-coarsening precipitates in the alloy at 750 °C.

4.2. Creep mechanisms

The different creep rate of the alloy in STD and SAACW state may be partially resulted from their different yield strength. In fact, the applied stress is higher than the yield strength of the STD alloy but lower than that of the SAACW alloy when the creep rate of the SAACW alloy is lower than that of the STD alloy. Alloy tested at stress level higher than yield strength should have high creep rate because it contains a great number of mobile dislocations produced by plastic deformation at the beginning.

It was reported that the thermal creep of V–4Cr–4Ti alloy at 800 °C/200 MPa was controlled by climb assisted dislocation glide [9]. The activation energy (Q) of the creep is equivalent to the self-diffusion activation energy of V atoms. Creep rate ($d\varepsilon/dt$) has a relationship with Q and the absolute temperature (T) as $d\varepsilon/dt = k\exp(-Q/RT)$, where k is a pre-exponential coefficient and R is gas constant of 8.314 kJ/mol. In the present study, the limited data only allow the estimation of the Q at the applied stress of 240 MPa. The reciprocal temperature dependence of the

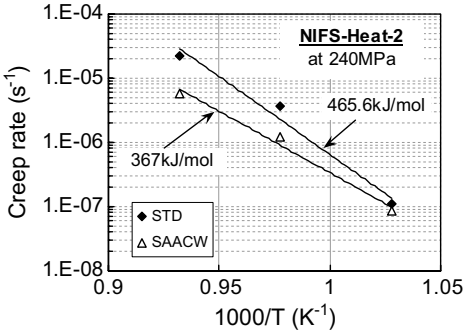

Fig. 8. The reciprocal temperature dependence of creep rate for the alloy tested at 240 MPa.

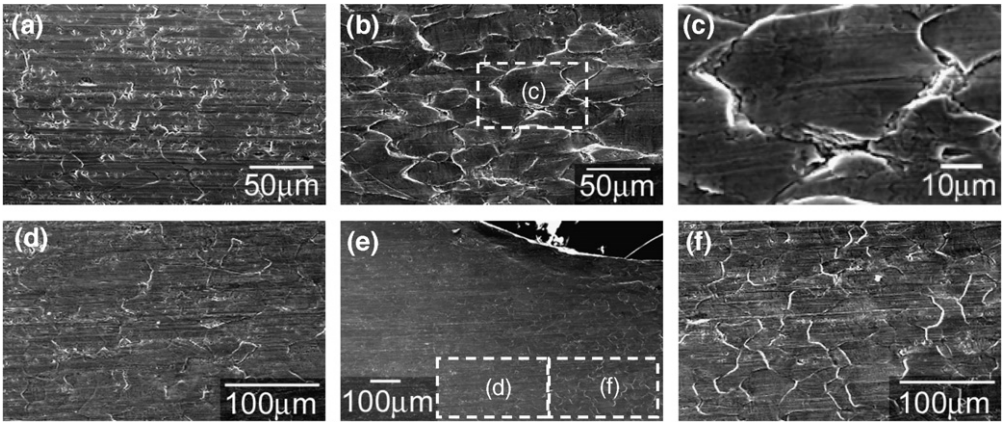

Fig. 9. SEM photos showing the SAACW specimen surface after creep test at (a) 700 °C/214 MPa/25 h (specimen was not ruptured) and (b)–(f) 800 °C/164 MPa/122 h (specimen was ruptured). Photo (c) is the magnification of the rectangular region in (b). Photo (d) and (f) are respectively the rectangular regions in (e). The corresponding ID characters were also indicated in the rectangular regions.

rate is shown in Fig. 8. According to the dependence, the estimated activation energy for the STD and the SAACW alloy were 465.6 and 367 kJ/mol, respectively, both are much higher than the self-diffusion energy of 270 kJ/mol of the alloy in the temperature range [9]. It seems that other mechanism than the dislocation climb controlled the creep deformation.

An observation with SEM showed the appearance of grain structure on the specimen surface after the creep test at 800 °C (see Fig. 9(b) and (c))) other than 700 °C (see Fig. 9(a)). The grain structures seemed to be a result of thermally etched grain boundaries during the high-temperature exposure in the vacuum environment. But cracks were observed along grain boundaries (see Fig. 9(c)), which should be caused by stress and deformation. Furthermore, grain structure clearly appeared only in the deformed region within the gauge section (photo (f)), while specimen end region without deformation (photo (d)) showed very weak trace. This appearance of the grain structure is thought to arise from grain boundary slide. Similar behavior was observed for the STD alloy.

There are many kinds of mechanisms for the creep deformation of V–4Cr–4Ti [10]. Possible mechanism here is the Coble creep, grain boundary slide controlled by vacancy diffusion, which could result in such trace and cracks along the grain boundaries.

5. Conclusions

The V–4Cr–4Ti alloy (NIFS-Heat-2) was thermomechanically treated to have higher strength by aging and cold rolling. The thermal stability of the strengthening was studied by annealing the alloy at 750 °C. TEM analysis was done to show the strengthening mechanisms. The high-temperature tensile properties and the uniaxial thermal creep behavior of the alloy were studied. Results were summarized as follows:

(1) Hardening the alloy by aging at 600 °C is very significant. Additional 20% cold rolling hardens the alloy further. The aging plus cold-rolling treated alloy has much higher tensile strength than the one treated according to the conventional standard annealing process up to 800 °C.
(2) The aging-produced fine precipitates got coarsening in the annealing at 750 °C. But the coarsening did not occur when the alloy contained high number density of dislocations that were introduced into the alloy by the cold rolling.
(3) The aging and cold rolling increased the resistance of the alloy to thermal creep at higher stress level than a critical value that seems to decrease with increasing temperature.
(4) The thermal creep at 800 °C seemed to be not controlled by dislocation climb but grain boundary diffusion or sliding.

Acknowledgements

This study was supported by Japan–China Core University Program and NIFS Budget Code NIFS06UCFF003 and NIFS06UCFF0011.

References

[1] Karl Ehrlich, E.E. Bloom, T. Kondo, J. Nucl. Mater. 283–287 (2000) 79.
[2] K. Sakai, M. Satou, M. Fujiwara, K. Takanashi, A. Hasegawa, K. Abe, J. Nucl. Mater. 329–333 (2004) 457.
[3] J.M. Chen, V–W–Ti alloys, Presented at the 7th IEA and JUPITER-II Joint Workshop on the Critical Issues for Vanadium Alloys for Fusion Application, December 15–16, 2003, Toki, Gifu, Japan.
[4] J.M. Chen, T. Muroga, T. Nagasaka, S.Y. Qiu, C. Li, Y. Chen, B. Liang, Z.Y. Xu, Fus. Eng. Des. 81 (2006) 2899.
[5] H.M. Chung, B.A. Loomis, D.L. Smith, Fus. Eng. Des. 29 (1995) 455.
[6] N.J. Heo, T. Nagasaka, T. Muroga, J. Nucl. Mater. 325 (2004) 53–60.
[7] T. Muroga, T. Nagasaka, K. Abe, V.M. Chernov, H. Matsui, D.L. Smith, Z.-Y. Xu, S.J. Zinkle, J. Nucl. Mater. 307–311 (2002) 547–554.
[8] T. Nagasaka, T. Muroga, A. Nishimura, J. Chen, K. Tokizawa, Development of a uniaxial creep testing machine for small specimen of low activation fusion reactor materials, Mater. Trans. (submitted for publication).
[9] K. Natesan, W.K. Soppet, A. Purohit, J. Nucl. Mater. 307–311 (2002) 585.
[10] R.J. Kurtz, US Program for Fusion Materials and Test Blanket Modules, presented in NIFS, Japan, July 13, 2006.
[11] A.F. Rowcliffe, S.J. Zinkle, D.T. Hoelzer, J. Nucl. Mater. 283–287 (2000) 508.